Chinese Chemical Letters 35 (2024) 109464

Contents lists available at ScienceDirect

Chinese Chemical Letters

journal homepage: www.elsevier.com/locate/cclet

Construction of wavelength-tunable DSE quinoline salt derivatives by regulating the hybridization form of the nitrogen atom and intramolecular torsion angle

Kuan Deng[a,1], Fei Yang[b,1], Zhi-Qi Cheng[a], Bi-Wen Ren[b], Hua Liu[a], Jiao Chen[a,b], Meng-Yao She[a,b,*], Le Yu[a], Xiao-Gang Liu[c], Hai-Tao Feng[d], Jian-Li Li[a,*]

[a] Key Laboratory of Synthetic and Natural Functional Molecule of the Ministry of Education, Shaanxi Key Laboratory for Carbon Neutral Technology, College of Chemistry & Materials Science, Northwest University, Xi'an 710127, China
[b] Key Laboratory of Resource Biology and Biotechnology in Western China, Ministry of Education; Biomedicine Key Laboratory of Shaanxi Province, Lab of Tissue Engineering, the College of Life Sciences, Faculty of Life Science & Medicine, Northwest University, Xi'an 710069, China
[c] Fluorescence Research Group, Singapore University of Technology and Design, Singapore 487372, Singapore
[d] Baoji AIE Research Center, Shaanxi Key Laboratory of Phytochemistry, College of Chemistry and Chemical Engineering, Baoji University of Arts and Sciences, Baoji 721013, China

ARTICLE INFO

Article history:
Received 25 October 2023
Revised 23 December 2023
Accepted 26 December 2023
Available online 30 December 2023

Keywords:
Fluorescence
Dual-state emission
Structure-function relationship
Wavelength regulation
Fluorescent imaging

ABSTRACT

Dual-state emission (DSE) molecules displayed conspicuous fluorescent performance both in solid and solution states. However, the construction of DSE molecules and the regulation of their emission wavelengths remains a great challenge. Based on the structure-function relationship of quinolinonitrile-type fluorophores, this work proposed a feasible strategy for modulating their fluorescent properties into DSE *via* limiting the torsion angle between the quinoline ring and C=C bond in the range of 4.7° to 30°. Based on this strategy, 53 compounds were obtained which displayed tunable emission wavelengths from 397 nm to 740 nm in solid-state and from 360 nm to 672 nm in solution. The feasibility of the strategy was supported by a series of theoretical calculations, optical characterizations, and crystal analysis, suggesting the compounds have great potential in imaging living cells and tissues with desired wavelengths.

The construction of fluorescent molecules with excellent performance draws lots of attention on account of their wide range of applications in optoelectronic materials [1–3], bioimaging [4–8], and medical diagnosis and treatment [9–13]. Traditional organic fluorescent materials generally have a highly rigid planar structure that tends to form π-π stacking in high concentration or solid-state, leading to aggregation-caused quenching (ACQ) phenomena which greatly limits their applications [13–15]. Encouragingly, in 2001, Tang *et al.* proposed aggregation-induced emission (AIE) [16] that has effectively broken through this limitation and greatly expanded the applications of organic fluorescent molecules, especially in the aggregated state [17–19]. However, AIE molecules commonly have highly distorted conformations that could enhance their molecular motion in a monomolecular state, leading to weak fluorescence in dilute solutions and further limiting the application in the solution state. Therefore, constructing dual-state emission (DSE) molecules both in solution and solid state is expected to fill the gap between ACQ and AIE molecules [20,21].

Some pioneering works about DSE have recently been reported [22–27]. For example, Tang and his co-workers proposed the concept of the conjugation-induced rigidity (CIR) strategy for the design of molecules with dual photoluminescence [28]. Dual-state emission can also be attained by incorporating bulk substituents into molecular structures to prohibit π-π stacking in the solid state [29–31]. However, there is no valid design strategy for designing DSE molecules because of the lack of an investigation into the relationship between structure and fluorescence performance [32]. In addition, the development of full-color and color-tunable organic luminophores is significant in terms of optoelectronic applications [33–35], such as optical devices, molecular switching, memory devices, and data storage, but the modulation of DSE properties was not reported so far. Thus, it is a big challenge to construct novel DSE molecules with controllable and tunable fluorescence spanning the whole visible region.

* Corresponding authors.
E-mail addresses: shemengyao@nwu.edu.cn (M.-Y. She), lijianli@nwu.edu.cn (J.-L. Li).
[1] These authors contributed equally to this work.

https://doi.org/10.1016/j.cclet.2023.109464
1001-8417/

In the previous report [36], Tian and co-workers described the main difference between typical AIE molecules (represented by quinolinemalononitrile, **AIE-1**) and the ACQ molecules (represented by dicyanomethylene-4*H*-pyran, **ACQ-1**) is the dihedral angle between benzoheterocycle and C=C plane, which was considered as an important reason for the different fluorescent characteristics in solvent-state and solid-state. The dihedral angle is smaller than 4.69° giving **ACQ-1** a planar structure, leading to weak solid-state fluorescence due to the ACQ effect. In contrast, the larger dihedral angle of 30.80° made **AIE-1** more tridimensional and greatly attenuated the intermolecular π-π stacking, resulting in enhanced solid-state fluorescence by the AIE effect.

Based on the above research, we suspected that regulation and control of the dihedral angle in a suitable region might be the key to constructing the desired DSE feature for this kind of molecule. The relatively large torsion angle in the molecule exhibits enhanced fluorescence in the solid state, and the relatively small torsion angle within the molecule exhibits enhanced fluorescence in the dilute solution. Furthermore, due to the specificity of the hybridization orbitals of nitrogen atoms in quinolinecarbonitrile (QM), the lone pairs of electrons are involved in bonding, and the atoms are arranged in the form of alternating single and double bonds, both of which adopt the sp^3 hybridization form, showing a largely distorted conformation. We speculate that the degree of distortion of the quinoline ring may be one of the factors affecting the size of the torsion angle between it and the C=C bond plane. Thus, we designed a series of platform structures using quinolinesulfonates as the core fluorophore and different benzaldehyde derivatives acting as the regulation moiety. Systematical fluorescent properties were investigated including wavelength, quantum yields, and lifetime in different states to reveal the structure-function relationship and verify the feasibility of this DSE fluorophore design strategy. Moreover, on this molecular platform, the full-color tunable character was also realized *via* the regulation of substituents. Compared with previously reported quinolinonitriles, the dinitrile moiety was removed from the molecule so that the hybridization form of N atom could convert from sp^3 into sp^2, resulting in a more complanate quinoline ring which might be beneficial for forming a small dihedral angle with C=C plane and showing DSE feature.

To logically regulate the torsion angle between the quinoline ring and the C=C bond in the molecule, we first investigated the structural characteristics of three representative structures quinolinonitrile, quinolone [37], and quinoline salts [38]. With the removal of dinitrile moiety, the hybridization form of the N atom changed from sp^3 to sp^2, giving decreased torsion angle and increased planarity. With the growth of the nitrogen alkyl chain, the distance of C1 from the quinoline ring was shortened, along with the warping degree of N away from the quinoline ring (Fig. S1 and Table S3 in Supporting information). Thus, we took **AIE-2** [39,40] as the core structure and removed malononitrile to increase the planarity of the quinoline unit and reduce the torsion angle between the quinoline ring and the C=C plane. **ACQ-1**, **AIE-1**, **AIE-2**, and seven more structures with different substituent groups were optimized *via* density functional theory (DFT) calculations (Fig. 1a and Table S4 in Supporting information). The torsion angle of **AIE-1** and **ACQ-1** is similar to their reported single-crystal structures. Importantly, the torsion angles in all these seven molecules displayed appropriate values of 4.7°–30° as expected, which are all smaller than 32.19° of **AIE-1** and larger than 0.68° of **ACQ-1** (Fig. S3 and Table S4 in Supporting information). Moreover, the quinolinium salt skeleton in these compounds exhibits more planar with a torsion angle (ab-ch) less than 1° compared to **AIE-1** and **ACQ-1**, which is beneficial for forming a conjugation-enhanced core structure. As a representative compound, **SN-Ben** was calculated to have good emission at 455.84 nm.

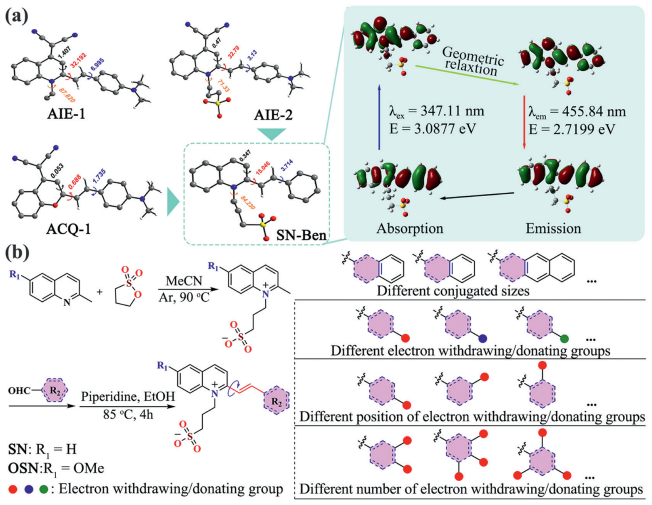

Fig. 1. (a) Optimized structures of **AIE-1**, **AIE-2**, **ACQ-1**, **SN-Ben**, and the calculated excitation/de-excitation wavelengths and the corresponding energies during the photoluminescence process of **SN-Ben**. (b) The synthesis of **SNs**/**OSNs** and the design of different substituents for the regulation of molecular structures and properties.

Encouraged by the simulation results, these molecules were facilely synthesized (Figs. 1b and 2) with good fluorescent emission both in dimethyl sulfoxide (DMSO) and solid state (Fig. 3a). Considering that quinoline salt was generally employed as a strong electron-withdrawing group to form asymmetric donor-acceptor (D-A) systems, solvents with different polarities including water, dimethyl sulfoxide, acetonitrile, methanol, ethanol, acetone, dioxane, tetrahydrofuran, and dichloromethane was used in the emission and absorption spectra experiments. As shown in Figs. 3b and c, Figs. S4–S16 (Supporting information), the absorption and emission spectra of these compounds all show minor redshift or blueshift variations (≈20 nm) at different solvent polarities due to the strong delocalization of the positive charge of the quinoline salt unit (Table S5 in Supporting information), indicating the polarity of solvent has a subtle influence on this kind of molecules and a very weak twisted intramolecular charge transfer (TICT) process [41]. Moreover, the emission peaks of these seven compounds could range from 492 nm to 737 nm in the solid state, suggesting excellent wavelength tunability in this platform.

Considering that almost all the maximum emission wavelengths of these six compounds in the solid state were larger than those in solution except **SN-9Ant**, a high possibility of *J*-type packing is speculated to exist in the solid state [42,43]. For **SN-9Ant**, the C=C bond forms a large torsion angle with the anthracene ring, weakening the effective conjugation strength of the molecule, resulting in weaker fluorescence emission and ultraviolet-visible absorption both in solid-state and solution (DMSO, ethanol, acetone, dioxane, tetrahydrofuran, and dichloromethane). As shown in Table S8 (Supporting information), the absolute fluorescence quantum yield is only 0.27% in the solid state and 1.70% in DMSO. According to the conjugation-induced rigidity effect (CIR) proposed by Tang *et al.*, the anthracene ring in the **SN-9Ant** molecule increases the rigidity of its distorted molecular conformation, eroding the integrity of molecular conjugation, and weakening its fluorescence intensity. Although the absolute fluorescence quantum yields of these compounds were generally low, the difference between solid and solution states for each molecule is not significant, indicating this type of structure possesses the properties of dual-state emission *via* controlling the torsion angle.

Interestingly, in this “push-pull” electron system, changing the substituent group into electron-donating units (-OMe, -NMe_2) on

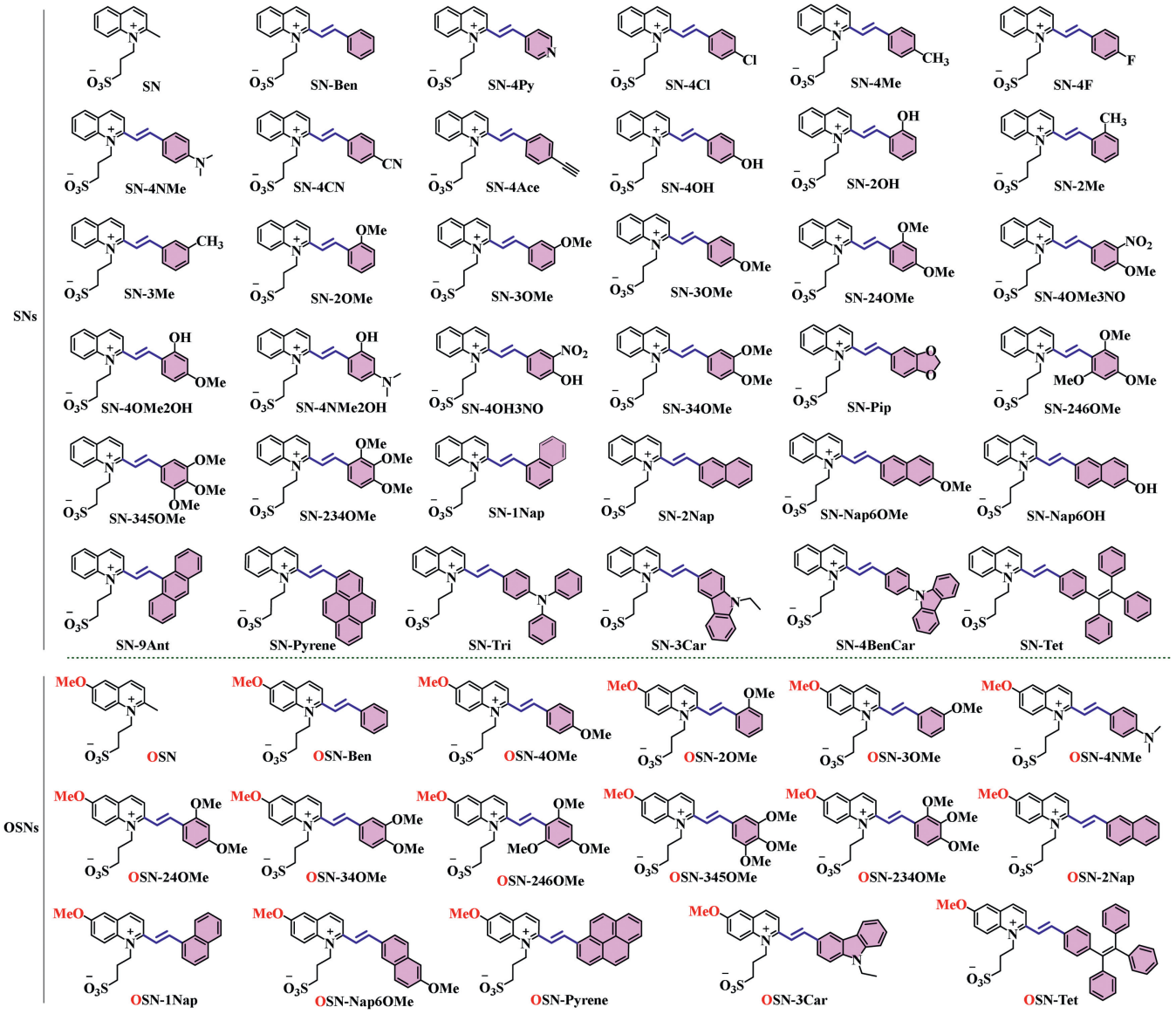

Fig. 2. Structures of all **SNs** and **OSNs**.

the *para*-position gives a significant redshift in the emission and absorption spectra in both solid and solution states, and the redshift degree is consistent with the electron-donating ability of the related substituent group. Moreover, with the phenyl ring replaced by increased conjugation systems such as naphthalene and anthracene ring, the redshift effect shows a positive correlation with the electron conjugation degree.

More universal quinoline sulfonate acetals **SNs** were further synthesized (Table S1 in Supporting information) and their fluorescent performance shown in Table S6 (Supporting information) also verifies that the above performance is widespread in this type of molecule. As expected, these quinoline sulfonate acetals **SNs** with various substitutional phenyl units manifested facile tunability on the emission and absorption wavelengths (Table S5 in Supporting information). As shown in Fig. S17 (Supporting information), the emission wavelengths can range from 397 nm to 737 nm in the solid-state and range from 360 nm to 672 nm in the DMSO solution, covering a wide spectral range reaching to NIR region. Along with the substitution of the electron donating/withdrawing group in the para-position of the phenyl unit, the maximum emission wavelength in the solid-state and solution is gradually redshifted. Similarly, expanding the conjugated system of the phenyl unit into alkyne, benzene, naphthalene, anthracene, or pyrene, giving the corresponding compounds **SN-4Ace**, **SN-2Nap**, **SN-9Ant**, and **SN-Pyrene**, could also extend the wavelength both in solid and solution states. Normally, as a "push-pull" electron system, the fluorescent properties were easy to be affected by the solvent with different polarity. Surprisingly, in this system, the compounds showed incredible stability of emission in diverse solvents including dichloromethane (DCM), tetrahydrofuran (THF), dioxane, acetone, ethanol, methanol, acetonitrile, DMSO, and water. Therefore, we have achieved a series of DSE fluorophores that covered full-wave band emission *via* controlling the torsion angle, whereafter, regulating the "push-pull" electron system and conjugation system.

To explore whether these features could be maintained when the electron distribution was changed, methoxy was introduced in the 6-position of quinoline salt giving 17 compounds **OSN**s (Fig. 2), and their spectral properties were also summarized in Table S6. In general, the fluorescent wavelength changing regularity of **OSN**s presented a similar redshift to that of the **SN**s upon the substitution of different electron donating/withdrawing groups. For conjugated system enhanced compounds, the maximum emission wave-

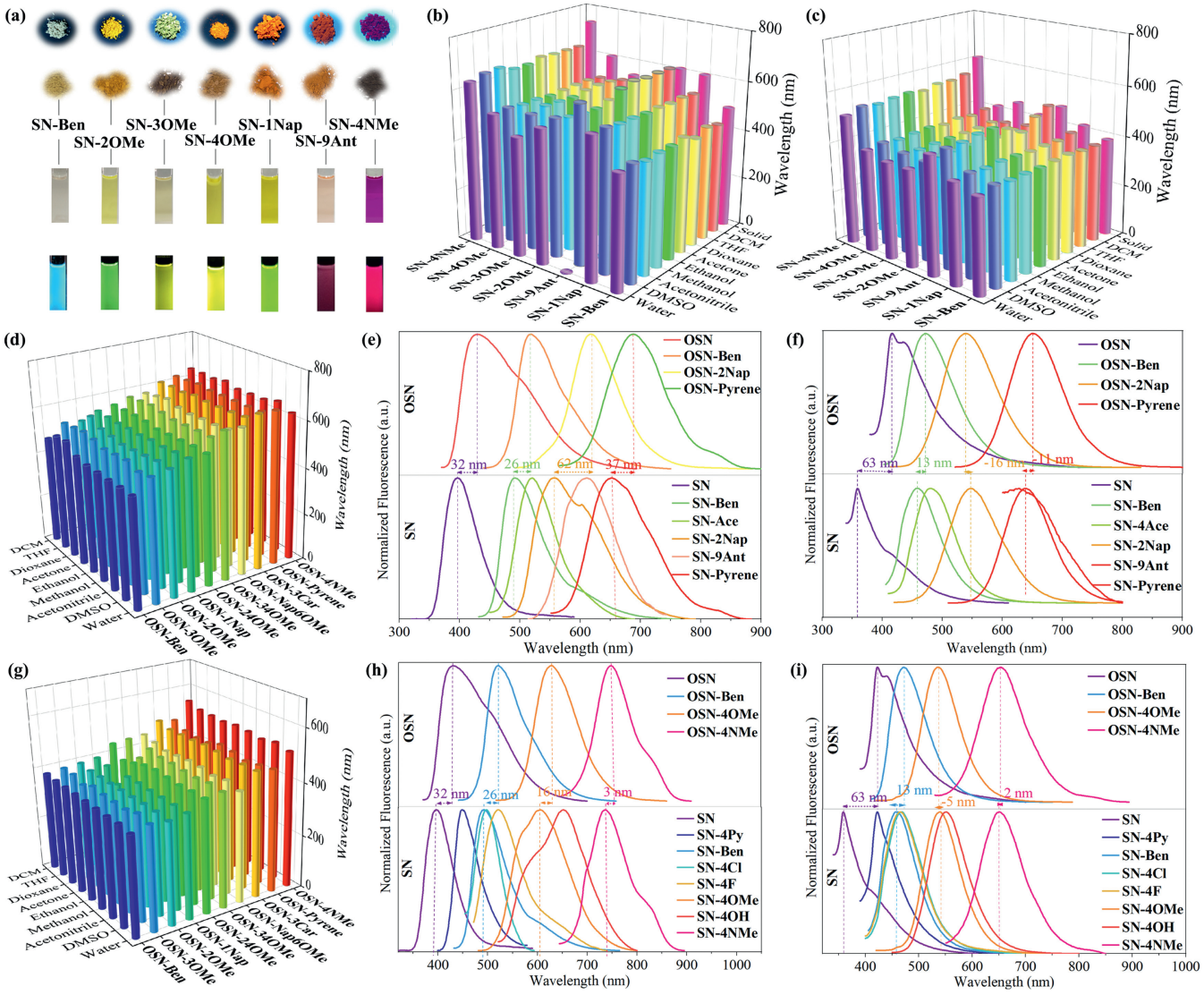

Fig. 3. (a) Photographs of the samples in the solid state and in DMSO (10^{-5} mol/L) under daylight and 365 nm excitation. (b) Maximum emission wavelengths and (c) maximum absorption wavelengths in solid state and different polar solvents and solids (10^{-5} mol/L). (d) The maximum emission wavelengths of **OSNs** in different solvents. (e) Emission wavelength regulating effect by the size of conjugated system in solid state. (f) Emission wavelength regulating effect by the size of conjugated system in DMSO. (g) The maximum absorption wavelengths of **OSNs** in different solvents. (h) Emission wavelength regulating effect by the electronic donating ability at the *para*-position in solid state. (i) E Emission wavelength regulating effect by the electronic donating ability at the *para*-position in DMSO.

length of **OSN**s is greater than the relevant **SN**s with the same substituted group due to the formation of a stronger D-A system (Figs. 3e and f). Interestingly, introducing methoxy in the 6-position of quinoline salt will produce more red emission than the corresponding **SN**s while their phenyl unit was substituted by a weak electron donating group. However, when the phenyl unit was replaced by a strong electron donating group such as **OSN-4NMe**, the emission-enhanced effect by the 6–methoxy became negligible (Figs. 3h and i). This indicated that the regulation of this specific molecular platform by the substitution of the quinoline core might be limited while the electron system was already highly polarized. However, for the polysubstituted compounds, the trend of the maximum emission wavelength of the **OSNs** and the **SNs** in the solid state is not exactly similar. When the phenyl was substituted by **234OMe**, the corresponding compounds **OSN-234OMe** displayed a longer emission of 30 nm over that of **SN-234OMe**. But when the substitute mode was changed to **345OMe**, the maximum emission wavelength showed 32 nm shorter than that of **SN-345OMe** (Fig. S15 in Supporting information). These results indicated that fluorescence control of this kind of molecule with polysubstituted form is not dominated by a single factor but determined by multiple factors (conjugative effect, electronic effect, steric effect) working in synergy. Similar to **SNs**, the introduction of methoxy in the 6-position of quinoline salt did not change the absorption and fluorescent stability in the solvent with different polarity, and the trend of compounds' wavelength change is also not influenced and still maintains a superior redshift gradient (Figs. 3d and g), indicating excellent anti-noise and robust performance.

The solid-state absolute fluorescence quantum yields of **OSNs** are generally higher than those of **SNs** with the same phenyl unit, indicating that the introduction of methoxy at position 6 might enhance the electron density and rigidity of the main structure (Table S8 and Fig. S25 in Supporting information). In solvent, the fluorescence quantum yield was gradually increased along with the enhancement of the conjugation system. Moreover, the distribution of fluorescence emission wavelengths for this series of compounds (Fig. S18 in Supporting information) was able to cover a very wide range, showing good wavelength tunability.

Furthermore, not only in the optimized structures but also in the single-crystal X-ray structures (Figs. S26–S44 and Tables S9–S13 in Supporting information), the flexible chain of the sulfonic acid group is inclined to approach the electron-rich C=C double bond giving relatively stable electrostatic attraction system. This specific pattern could improve the rigidity, maintain the twisted conformation, and reduce intramolecular rotation caused by energy dissipation, leading to a series of positive fluorescent properties enhancement. Thus, these specific structural features generated from the modulation of the torsion angle might be the predominant factor in regulating the fluorescent properties to be DSE between the critical values of AIE and ACQ.

Taking **SN-3OMe** and **OSN-3OMe** as examples, the torsion angle was only displayed as slightly different, indicating that the substituent of the methoxy group at position 6 of the quinoline unit had almost no effect on the degree of torsion. But comparing **OSN-2OMe** with **OSN-3OMe**, the torsion angle showed a non-negligible increase possibly caused by the steric effect. Moreover, this steric effect might also keep the flexible N-propyl sulfonic acid chain away from the C=C bond as illustrated in the optimized geometrical configuration and single crystal structure. Compared with the benzene ring, the anthracene ring in compound **SN-9Ant** has a larger rigid plane and displayed a larger steric effect, resulting in an excessive torsional angle between the central C=C bond and the anthracene ring (47.57°). Affected by the above-mentioned reason, the torsion angle between the central C=C bond and the quinoline salt unit was derived to 33.55°, which greatly weakened the effective conjugated degree and reflected in the relatively unsatisfactory fluorescent performance. Thus, in this particular platform, the torsion angle was mainly controlled by the following factors: (i) the orientation of the N-propyl sulfonate group, (ii) the planarity of quinoline unit, and (iii) the substituent form of phenyl unit. The molecular fluorescent performance is capable of modulation *via* these indicators.

Moreover, since the C=C bond was formed at different torsion angles with the quinoline ring and phenyl respectively, the dihedral angle between the quinoline ring and phenyl unit was limited between 6.5° (**ACQ-1**) and 47.5° (**AIE-1**). This distorted conformation forced the quinoline unit to overlap with the phenyl group in the stacking mode, giving the closest intermolecular distance from 3.60 Å to 4.40 Å, which was larger than the general π-π interaction distance. Owing to the *N*-propyl sulfonate group and twisted molecular structure, no effective overlap of the π-π surface was observed in all crystal structures. More importantly, special dimers with antiparallel and slip-stacked alignment were formed in the crystal, which is similar to Z-type and consistent with the optical feature, indicating a possible *J*-aggregation mode. The large Stokes shift and relevant strong fluorescence in the solid state also verify the aggregation mode. It is worth noting that when the hydrogen at the 6th position of the quinoline unit was replaced by methoxy, weak C–H···O–CH_3 (2.57 Å to 2.87 Å) interactions were observed, which might enhance the intermolecular rigidity and suppress the rotation or motion of **OSNs** molecules, leading to enhanced emission intensity and quantum yields in the solid state.

Furthermore, the biological fluorescent imaging performance was investigated using **SN-345OMe** as an example considering its relatively larger emission wavelength and large Stokes shift. First, the compound was examined to be low cytotoxicity by cell counting kit-8 (CCK8) assay (Fig. S45 in Supporting information). As shown in Fig. 4a, bright fluorescence in the red channel of 293T cells was observed after incubation for 20 min. More importantly, **SN-345OMe** was confirmed to mainly stay in lysosomes based on the good Pearson coefficient of 0.947 with commercial Lyso-Tracker Green. Moreover, **SN-345OMe** was also capable of sketching the boundary and detailed structures of the heart, kidney, liver, lung, and spleen, suggesting that this kind of compound could serve as promising biological fluorescent probes in the imaging of cells and tissues (Fig. 4b). All the animal experiments have been approved by the Animal Ethics Committee of Northwest University (NWU-AWC-20220408 M).

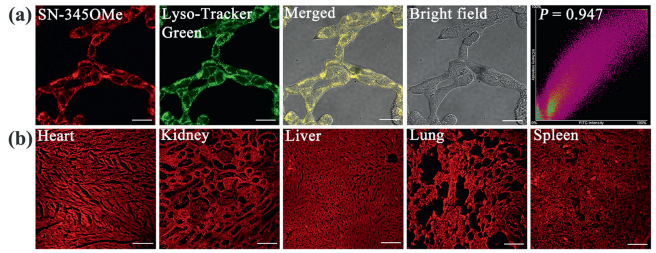

Fig. 4. (a) Fluorescent imaging of 293T cells incubated with **SN-345OMe** (λ_{ex} = 543 nm), Lyso-Tracker Green (λ_{ex} = 488 nm), the overlaid image between the red and green channels, the bright field image, and the pixel correlation plot (Scale bar: 25 μm). (b) Heart, kidney, liver, lung, and spleen imaging of BALB/c mice incubated with **SN-345OMe** (λ_{ex} = 543 nm, scale bar: 100 μm).

In conclusion, we have achieved a promising design strategy for two series of DSE molecules **SNs** and **OSNs** *via* converting quinoline N from sp^3 to sp^2 and adjusting the torsion angle between the AIE and ACQ fragments on the quinoline salt platform. The fluorescence wavelengths of the synthesized DSE molecules could be regulated from 397 nm to 740 nm in solid-state and from 360 nm to 656 nm in solution by changing the substitution pattern in the phenyl unit. Moreover, the compounds exhibited excellent fluorescent imaging ability in living cells and different tissues. This work would provide a feasible way for the construction of new DSE organic fluorescent dyes and show its potential in the application of fluorescent materials with the desired wavelengths.

Declaration of competing interest

The authors declare that they have no known competing financial interests or personal relationships that could have appeared to influence the work reported in this paper.

Acknowledgments

This work was supported by the National Natural Science Foundation of China (Nos. 22077099 and 22171223), The Innovation Capability Support Program of Shaanxi (Nos. 2023-CX-TD-75 and 2022KJXX-32), the Scientific and Technological Innovation Team of Shaanxi Province (No. 2022TD-36), the Technology Innovation Leading Program of Shaanxi (No. 2023KXJ-209), the Natural Science Basic Research Program of Shaanxi (Nos. 2023-JC-YB-141 and 2022JQ-151), and Young Talent Fund of Association for Science and Technology in Shaanxi, China (No. SWYY202206), the Shaanxi Fundamental Science Research Project for Chemistry & Biology (Nos. 22JHZ010 and 22JHQ080), the Yan'an City Science and Technology Project (No. 2022SLZDCY-002).

Supplementary materials

Supplementary material associated with this article can be found, in the online version, at doi:10.1016/j.cclet.2023.109464.

References

[1] Y. Qin, Q. Ling, Y. Wang, et al., Angew. Chem. Int. Ed. 62 (2023) e202308210.
[2] M. Dai, B. Zhou, X. Fang, et al., ACS Appl. Mater. Interfaces 14 (2022) 40223–40231.
[3] Q. Xu, L. Ma, X. Lin, et al., Chin. Chem. Lett. 33 (2022) 2965–2968.
[4] K. Ma, H. Yang, X. Wu, et al., Angew. Chem. Int. Ed. 62 (2023) e202301518.
[5] L. Wang, J. Liu, M. Ren, et al., Chin. Chem. Lett. 35 (2024) 108945.
[6] C. Wang, W. Jiang, D. Tan, et al., Chem. Sci. 14 (2023) 4786–4795.

[7] Y. Chen, H. Zhang, Y. Liu, et al., ACS Sens. 8 (2023) 2359–2367.
[8] X. Tian, D. Wu, W. Wei, et al., Chin. Chem. Lett. 35 (2024) 108912.
[9] B. Li, H. Liu, Y. He, et al., Angew. Chem. Int. Ed. 61 (2022) e202200025.
[10] Y. Yang, M. Ma, L. Shen, et al., Angew. Chem. Int. Ed. 62 (2023) e202310408.
[11] X. Ma, Y. Huang, W. Chen, et al., Angew. Chem. Int. Ed. 62 (2023) e202216109.
[12] Y. Chen, C. Xue, J. Wang, et al., Chin. Chem. Lett. 33 (2022) 1637–1642.
[13] B. Huang, X. Liu, G. Yang, et al., CCS Chem. 4 (2021) 2090–2101.
[14] E. Feng, L. Jiao, S. Tang, et al., Chem. Eng. J. 432 (2022) 134355.
[15] N. Ahmed, W. Zareen, Y. Ye, Chin. Chem. Lett. 33 (2022) 2765–2772.
[16] J. Luo, Z. Xie, J.W.Y. Lam, et al., Chem. Commun. (2001) 1740–1741.
[17] L. Liu, C. Li, J. Gong, et al., Angew. Chem. Int. Ed. 62 (2023) e202307776.
[18] T. Zhang, X. Chen, C. Yuan, et al., Angew. Chem. Int. Ed. 62 (2023) e202211550.
[19] Z. Li, S. Chen, Y. Huang, et al., Chem. Eng. J. 450 (2022) 138087.
[20] J.L. BelmonteVázquez, Y.A. AmadorSánchez, L.A. RodríguezCortés, et al., Chem. Mater. 33 (2021) 7160–7184.
[21] L.A RodríguezCortés, A. NavarroHuerta, B. RodríguezMolina, Matter 4 (2021) 2622–2624.
[22] W. Dai, P. Liu, S. Guo, et al., ACS Appl. Bio Mater. 2 (2019) 3686–3692.
[23] M. Huang, J. Zhou, K. Xu, et al., Dyes Pigm. 160 (2019) 839–847.
[24] Y. Li, Y. Lei, L. Dong, et al., Chem. Eur. J. 25 (2019) 573–581.
[25] Q. Qiu, P. Xu, Y. Zhu, et al., Chem. Eur. J. 25 (2019) 15983–15987.
[26] X. Zhang, Y. Zhou, M. Wang, et al., Chem. Asian J. 15 (2020) 1692–1700.
[27] X. Hu, A.C. Sedgwick, D.N. Mangel, et al., J. Am. Chem. Soc. 144 (2022) 7382–7390.
[28] G. Chen, W. Li, T. Zhou, et al., Adv. Mater. 27 (2015) 4496–4501.
[29] S. Qu, Q. Lu, S. Wu, et al., J. Mater. Chem. 22 (2012) 24605–24609.
[30] A. Shundo, Y. Okada, F. Ito, et al., Macromolecules 45 (2012) 329–335.
[31] H. Wu, Z. Chen, W. Chi, et al., Angew. Chem. Int. Ed. 58 (2019) 11419–11423.
[32] X. Mei, J. Wang, Z. Zhou, et al., J. Mater. Chem. C 5 (2017) 2135–2141.
[33] D.C. Green, J. Ihli, P.D. Thornton, et al., Nat. Commun. 7 (2016) 13524.
[34] T. Ma, T. Li, L. Zhou, et al., Nat. Commun. 11 (2020) 1811.
[35] Z. Wang, X. Wang, S. Cong, et al., Nat. Commun. 11 (2020) 302.
[36] C. Shi, Z. Guo, Y. Yan, et al., ACS Appl. Mater. Interfaces 5 (2013) 192–198.
[37] L.G. Kuz'mina, A.G. Sitin, E.N. Gulakova, et al., Crystallogr. Rep. 56 (2011) 611–621.
[38] J.E. Nycz, K. Czyż, M. Szala, et al., J. Mol. Struct. 1106 (2016) 416–423.
[39] A. Shao, Z. Guo, S. Zhu, et al., Chem. Sci. 5 (2014) 1383–1389.
[40] W. Fu, C. Yan, Z. Guo, et al., J. Am. Chem. Soc. 141 (2019) 3171–3177.
[41] F. Xiao, X. Liu, K. Lin, et al., J. Phys. Chem. C 125 (2021) 16792–16802.
[42] M. Huang, R. Yu, K. Xu, et al., Chem. Sci. 7 (2016) 4485–4491.
[43] C. Maeda, T. Todaka, T. Ueda, et al., Chem. Eur. J. 22 (2016) 7508–7513.